ACS APPLIED MATERIALS & INTERFACES

Research Article

www.acsami.org

Molecular Simulation for Gas Adsorption at NiO (100) Surface

Baochang Wang,*[,†] Jawad Nisar,[‡] and Rajeev Ahuja[†,‡]

[†]Applied Materials Physics, Department of Materials and Engineering, Royal Institute of Technology (KTH), S-100 44 Stockholm, Sweden

[‡]Condensed Matter Theory Group, Department of Physics and Astronomy, Box 516, Uppsala University, 751 20 Uppsala, Sweden

ABSTRACT: Density functional theory (DFT) calculations have been employed to explore the gas-sensing mechanisms of NiO (100) surface on the basis of energetic and electronic properties. We have calculated the adsorption energies of NO_2, H_2S, and NH_3 molecules on NiO (100) surface using GGA+U method. The calculated results suggest that the interaction of NO_2 molecule with NiO surface becomes stronger and contributes more extra peaks within the band gap as the coverage increases. The band gap of H_2S-adsorbed systems decrease with the increase in coverage up to 0.5 ML and the band gap does not change at 1 ML because H_2S molecules are repelled from the surface. In case of NH_3 molecular adsorption, the adsorption energy has been increased with the increase in coverage and the band gap is directly related to the adsorption energy. Charge transfer mechanism between the gas molecule and the NiO surface has been illustrated by the Bader analysis and plotting isosurface charge distribution. It is also found that that work function of the surfaces shows different behavior with different adsorbed gases and their coverage. The work function of NO_2 gas adsorption has a hill-shaped behavior, whereas H_2S adsorption has a valley-shaped behavior. The work function of NH_3 adsorption decreases with the increase in coverage. On the basis of our calculations, we can have a better understanding of the gas-sensing mechanism of NiO (100) surface toward NO_2, H_2S, and NH_3 gases.

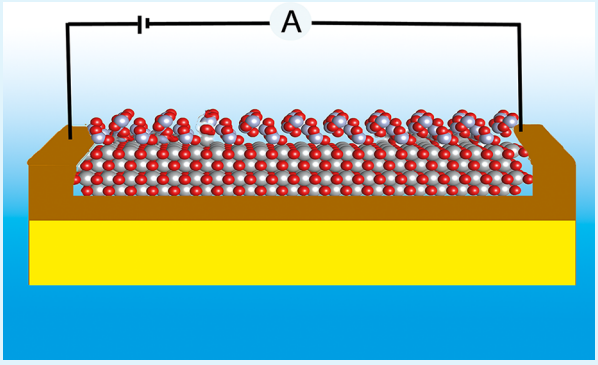

KEYWORDS: *gas sensing, NiO (100) surface, density functional theory (DFT), conductivity*

INTRODUCTION

Metal oxides semiconductors have been considered as a solid-state gas-sensing materials during the past few decades,[1] because of their stability and surface reactivity at the operation conditions. It is well-known that the electronic structure of the metal oxides changes with the adsorption of different gas molecules, which is the detecting parameter for gas sensing. According to the conductance mechanism for gas sensing, two different kinds of conductors can be distinguished.[2] The first one is ion conductors such as ZrO_2 and CeO_2, working as a membrane, separating two gases with differing chemical potentials. The other one is the semiconductors with n- or p-type conduction mechanism, which can detect electrical conductivity response to oxidize or reduce gases. Many gas-sensing materials are based on n-type semiconductors. Gas sensors based on SnO_2, ZnO, In_2O_3, and TiO_2 are n-type conduction response and have been widely investigated for detecting toxic gases. Nickel oxide (NiO) is considered as a model p-type metal oxide material because of its good chemical stability and excellent electrical properties.[3,4] NiO (100) surface is one of the promising reactive surfaces with wide band gap ranging from 3.6 to 4.0 eV with good optical and magnetic properties. Experimentally, nanocrystalline NiO thin films is fabricated by sputtering, pulsed laser deposition, or sol−gel technology, which has been proved to be a promising gas sensing material for various gases such as NO_2,[5,6] H_2S,[5] CO,[7] NH_3,[8] H_2,[9−13] and HCHO (formaldehyde).[14,15]

The gas-sensing mechanism of sensors involves adsorption of gas molecules on the metal oxide semiconductor surfaces and charge transfer between the semiconductor surfaces and the adsorbed molecules, leading to changes in its charge carrier concentrations and electrical conductivity.[16] When a n-type semiconductor, with majority charge carriers of electrons, is exposed to oxidizing gases such as NO_2, which have the ability to withdraw charge from the surface, its charge carriers will be decreased. However, the reducing gases such as H_2S can denote charges to the surface with the increase of charge carriers. For a p-type semiconductor, positive holes work as its majority charge carriers, and opposite effects are observed with an increase in conductivity in the presence of oxidizing gases and vice versa. In general, the conductivity of a material is increased with the increase of the carrier concentration as more carriers are available for conduction. On the contrary, conductivity decreases with the decrease in available carriers. In this way, electrical conductivity of the sensors plays as sensing parameter for gas sensors.[17] The adsorption process of molecules at the surface can be computed by ab initio calculations, which have

Received: August 17, 2012
Accepted: October 1, 2012
Published: October 1, 2012

 © 2012 American Chemical Society dx.doi.org/10.1021/am3016894 | ACS Appl. Mater. Interfaces 2012, 4, 5691−5697

been proven to be a useful tool to understand the gas-sensing mechanism at atomic level.

For many transition metal oxides, generalized gradient approximations (GGA) of density functional theory (DFT) fails to predict the correct electronic structure because of the strong correlation effects. The rotationally invariant version of the GGA+U method can give a good description of the cohesive energy, electronic structure, and mechanical and magnetic properties of NiO bulk and the surfaces.[18−21] In the recent work, it has been observed that GGA+U method can give good prediction for the adsorption of CO and NO molecules at the NiO (100) surface.[20,21] Thus, we have employed GGA+U method to study the energetic, electronic properties, and charge transfer mechanism to elucidate the adsorption of NO_2, H_2S, and NH_3 gas molecules at NiO (100) surface. The adsorption energies of different gas molecules on the NiO (100) surface are calculated for various coverage. In the current study, the electronic properties and charge-transfer mechanism have been considered and predicted the parameters, which play an important role in the gas-sensing process.

COMPUTATION METHODS

In the present study, the total energy and electronic-structure calculations were carried out within the framework of the spin-density-functional theory using the projected augmented wave (PAW) method,[22] as implemented in the Vienna Ab initio Simulation Package (VASP) package.[23−25] The PAW potentials with the valence states 4s 3d for Ni, 2s 2p for O and N, 3s 3p for S, and 1s for H have been employed. The exchange-correlation interaction was treated in the level of the Perdew−Burke−Ernzerhof (GGA-PBE) exchange correlation functional.[26] The Brillouin zone was sampled using Monkhorst-Pack generated set of k-points.[27] K-points mesh of 4 × 4 × 1 was found to be sufficient to reach convergence criteria for both the energy and the forces. The plane cutoff of the energy of 500 eV was used to describe the electronic wave function. The rotationally invariant version of the GGA+U method introduced by Lichtenstein et al.[18] has been used for our calculations. The parameter U was chosen to be 6.3 eV with the reference of previous studies.[20,21] The NiO (100) surface was reconstructed by the periodic repeated slabs with four atomic layers thick, which was separated by 15 Å vacuum. The gas molecules and the top two layers of NiO (100) were relaxed and the remaining two layers were fixed. One, two, and four gas molecules have been placed at the p (2 × 2) surface to model the 0.25, 0.5, and 1 monolayer (ML) molecular adsorption.

RESULTS AND DISCUSSION

Bare NiO (100) Surface. First of all, we have reconstructed the NiO (100) surface, which is nonpolar and the most stable surface. Crystal structure of NiO (100) surface is presented in Figure 1, which has four possible adsorption sites labeled. The electronic structure of the bare NiO (100) surface is investigated for the basic understanding of gas-sensing applications. The magnetic ordering in the (100) surface plane is antiferromagnetic, which confirms the previous study.[28,29] The electronic structure of bare NiO (100) surface is described by plotting the total and partial density of states (Figure 2), which clearly shows that the NiO (100) slab is antiferromagnetic with the band gap, 2.48 eV and the local magnetic momentum 1.71 μ_B, which is in good agreement with the recent work.[20] According to the partial density of states of surface Ni atom, two well-separated sub bands of the t_{2g} states is observed, and the peak at the conduction band edge originates from d_{z^2} states, which is only subject to the field generated from the oxygen atoms below the Ni surface atom. The crystal field felt by $d_{x^2-y^2}$ orbital does not change, as compared to the bulk. This might be the reason that the band gap of the NiO (100) surface is lower than the bulk.[20,30]

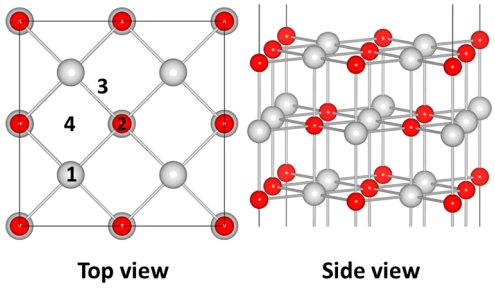

Figure 1. Crystal structure of NiO (100) surface top view and side view and possible reactive sites are labeled in top view.

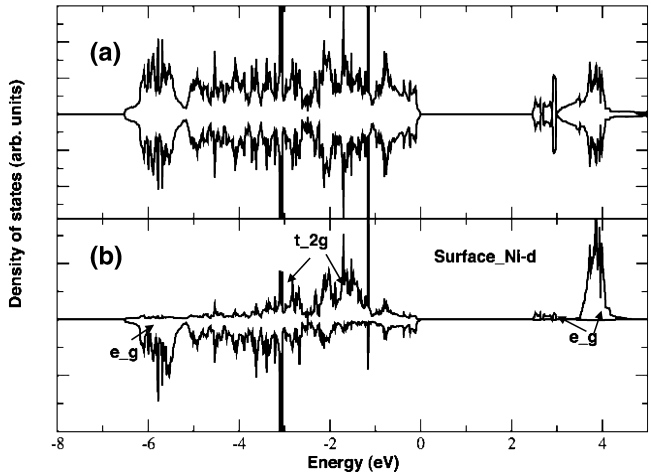

Figure 2. (a) Total density of states of NiO (100) surface and (b) the projected density of states of Ni 3d states for nickel ions of surface layer. Fermi energy is set to zero.

We have investigated the adsorption behavior of gas molecules such as NO_2, NH_3, and H_2S, using spin polarized generalized gradient approximations (SGGA) +U methods with U = 6.3 eV, the same value for the bare NiO (100) surface has been used. Four possible reactive sites are considered on the NiO (100) surface: top of Ni atom (site 1), top of O atom (site 2), bridge site (site 3), and hollow site (site 4), labeled in Figure 1. The energies of the gas molecule placed at all possible reactive sites have been calculated and the most favorable adsorption site for each gas molecule is chosen by energetic analysis. Both H_2S and NO_2 planar molecule have been put perpendicular to the surface plane with S and N downward, whereas the NH_3 molecular is put at the surface with N atom close to the surface. The initial adsorption configurations with NO_2 and H_2S parallel to the surface plane have also been studied. We have varied the adsorption coverage for each molecular on NiO (100) surface because the gas sensing properties are much related to the coverage. For further investigation of the adsorption of molecules on the surface, we have calculated the adsorption energy (E_{ads}), which is defined as[31,32]

$$E_{ads} = \frac{E[\mathrm{NiO} + \mathrm{nM}] - E[\mathrm{NiO}] - nE[\mathrm{M}]}{n} \quad (1)$$

Where the E[NiO + nM], E[NiO], and E[M] are the total energies of the molecules adsorbed on NiO (100) surface, the NiO (100), and the molecules. n indicates the number of adsorbed molecules at the surface.

Adsorption of NO_2. We have considered the adsorption of the NO_2 at the NiO (100) surface, the adsorption energy of system with different coverage is listed in Table 1. The NO_2 molecule adsorption on NiO (100) surface is found to be an exothermic process with adsorption energies of −0.36, −0.51, and −0.31 eV per molecule for 0.25, 0.5, and 1 ML coverage, respectively. In the case of 0.25 ML coverage, the NO_2 molecule changes its initial adsorption configuration and tilts toward the surface with one of its oxygen binding to the surface of Ni atoms (bond length of Ni−O is 2.19 Å). The NO_2 molecule sits at the surface hollow site with O and N atoms lying in the plane parallel to the NiO (100) surface (shown in Figure 3a). Bond angle of the NO_2 molecule is reduced to 125.9° after optimization as compared to the neutral gas molecule (133.4°), but close-to-surface N−O bond length of NO_2 molecule is stretched to 1.25 Å with respect to the 1.22 Å in its equilibrium gas phase. When we increase the gas molecule coverage to 0.5 ML, gas molecules are attached more strongly as compared to the 0.25 ML, which is also confirmed from the adsorption energy (−0.51 eV/molecule). The adsorption site is at the top of the Ni atom and each molecular plane is perpendicular to the surface (Figure 3b). The distance between the O atom of NO_2 and the surface Ni atom is 2.07 Å, which is slightly shorter than that of the 0.25 ML adsorption and even shorter than the bond length of the bulk material (2.10 Å). The bond length of N−O and bond angle of the NO_2 molecules are not changed significantly as compared to the free molecule.

Table 1. Adsorption Energies and Band Gap for the Adsorption of NO_2, H_2S, and NH_3 Molecules on NiO (100) Surface at Different Coverage Using GGA+U Method

gas molecules	coverage (θ)	adsorption energy (eV/molecule)	band gap (eV)
bare NiO			2.48
NO_2	0.25	−0.360	1.9
	0.5	−0.505	
	1	−0.310	
H_2S	0.25	−0.060	2.42
	0.5	−0.059	2.32
	1	−0.082	2.45
NH_3	0.25	−0.332	2.24
	0.5	−0.270	1.76
	1	−0.101	1.94

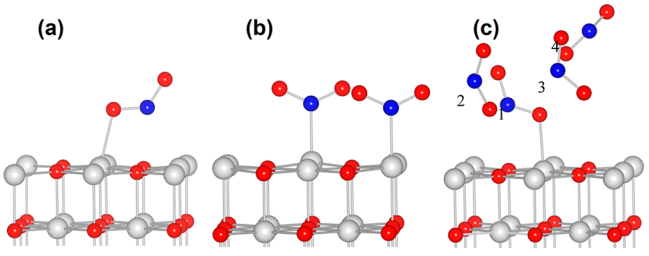

Figure 3. Adsorption of NO_2 molecules adsorbed on NiO (100) surface with different coverage: (a) 0.25 ML, (b) 0.5 ML, and (c) 1 ML after relaxation. Ni, O, and N atoms are represented by gray, red, and blue spheres, respectively.

For 1.0 ML coverage, the four NO_2 molecules are adsorbed at the surface. The first molecule is tilted toward the surface with one of its oxygen bond to the surface Ni atom, showing strong interaction, but other molecules are slightly repelled and weakly interact with the surface. The bond length of Ni−O is 2.08 Å for the first NO_2 molecule, which is comparable with the bond length of bulk material (2.10 Å). The N−O bond close to the surface is stretched to 1.25 Å, the same as in the low coverage system. The second NO_2 molecule sits on top of surface Ni atom with distance more than 3 Å from surface, which have no strong interaction with the surface. The third and fourth NO_2 come close to each other, forming an additional N−O bond with a length of 1.88 Å. At high coverage, we infer that physisorption and chemisorption phenomena both exist at the NiO (100) surface for the formation of a second ad-layer of NO_2 molecules (Figure 3c). The lower adsorption energy per molecule (−0.31 eV) is obtained in the case of 1 ML, which is due to the fact that half of the molecules bound weakly to the surface. The stronger interactions of the NO_2 gas with surface lower sensor response due to the removal of the adsorbed molecules become more difficult, which is in good agreement with previous experimental result.[5]

The electronic structure of the adsorbed system has been changed with respect to bare NiO surface due to the interaction between the NO_2 molecule and the NiO (100) surface. Density of states have been plotted to explain the electronic structure of adsorbed systems (shown in Figure 4a). Unoccupied states appear just above the Fermi level and at the tail of the valence band, which changes the electronic properties of the NiO surface. NiO surface is very sensitive for NO_2 gas sensing

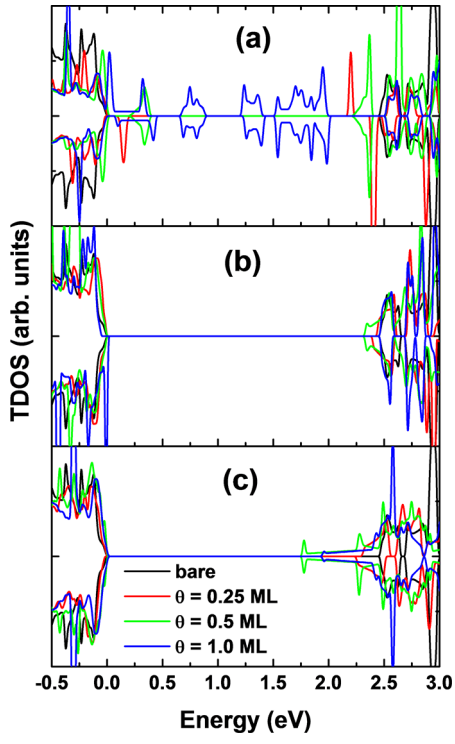

Figure 4. Total density of states (TDOS) of NiO (100) surface with the adsorption of (a) NO_2, (b) H_2S, and (c) NH_3 molecules at the surface. Fermi energy is set to zero.

dx.doi.org/10.1021/am3016894 | ACS Appl. Mater. Interfaces 2012, 4, 5691−5697

because of high adsorption energy and drastic change of the electronic structure. Concentration of impurity states in the band gap increases with the increase of NO_2 coverage. Partial filled states appear at the Fermi level, which shows the metallic behavior. Thus, it is observed that the electronic property of the surface has been changed from semiconductor to metal at high NO_2 concentration.

To study the bonding and charge transfer mechanism of NO_2 molecule at NiO surface, we have plotted the partial density of states of 0.5 ML coverage in Figure 5. It indicates that the main

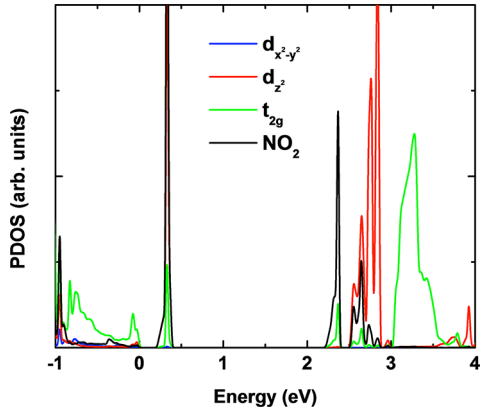

Figure 5. Partial density of states (PDOS) of surface Ni 3d states and the total density of states of NO_2 molecule. Fermi energy is set to zero.

interaction between the molecule and surface comes from the hybridization of Ni d_{z^2} and NO_2 HOMO states. The LUMO (lowest unoccupied molecular orbital) level of NO_2 is hybridized with the t_{2g} states. NO_2 molecule is found strongly bind to the surface Ni atom. $0.27e^-$ and $0.413e^-$ charges are transferred from the Ni atom to the NO_2 molecule for 0.25 and 0.5 ML coverage, respectively. To understand the bonding of NO_2 adsorption at NiO (100) surface, electron density difference $\Delta\rho = \rho_{(NiO:NO_2)} - (\rho_{NiO} + \rho_{NO_2})$ is calculated, which illustrates how the charge density changes during this adsorption process. Figure 6 shows the isosurfaces of differential charge density of the NO_2 molecule adsorbed on NiO (100) surface. Here the charge density can be either positive (depletion) or negative (accumulation), depending on whether an atom gains or loses charge. It is observed that the

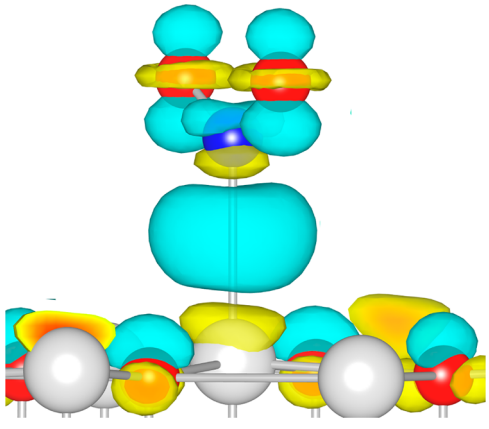

Figure 6. Isosurface of differential charge density of NO_2 gas molecule adsorbed at NiO (100) surface (yellow, depletion; cyan, accumulation) (isovalue = 0.004 e/Å^3).

interaction between surface Ni atom and NO_2 molecular makes the depletion of the Ni d_{z^2} states.

Adsorption of H_2S. In this part of the paper, we have also considered the H_2S molecules at NiO (100) surface for gas sensing, the stable adsorption site is on the top of the Ni atom with the molecular plane parallel to the surface. After relaxation, the distance between S atom of the H_2S molecule and the surface Ni atom is 2.57 Å. Geometry of H_2S molecules is not distorted after adsorption because the interaction between adsorbates and substrate is weak. The H_2S molecule adsorption on NiO (100) surface is also found to be an exothermic process with adsorption energies of −0.06, −0.06, and −0.08 eV per molecule for 0.25, 0.5, and 1 ML coverage, respectively, which is quite lower than the NO_2 adsorption. It looks like the physisorption interaction between the molecule and the surface. It indicates that adsorption energy remains almost constant with different coverage. The weak interactions increase the sensor response time because the removal of the adsorbed molecules is easier than NO_2. In the case of 0.5 ML, one molecule is closer to the surface with the bond length of 2.6 Å, whereas the second molecular moves away from the surface with the distance of 3.05 Å. The second molecule has a smaller title with the angle of 60° between molecular plane and surface plane. Here, geometry of the H_2S molecule is not changed because of very weak interaction (shown in Figure 7a, b)

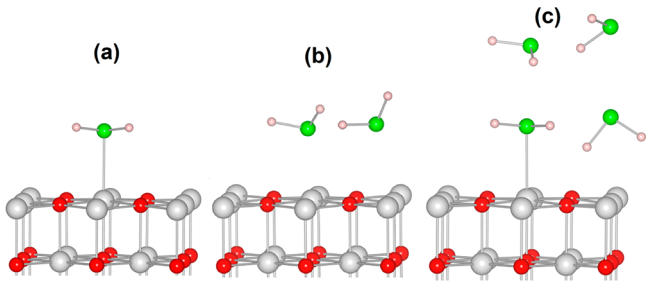

Figure 7. Adsorption of H_2S molecules adsorbed on NiO (100) surface with different coverage: (a) 0.25 ML, (b) 0.5 ML, and (c) 1 ML after relaxation. Ni, O, S, and H atoms are represented by gray, red, green, and white spheres, respectively.

We have also studied monolayer coverage of H_2S at NiO (100) surface. After the atomic optimization, half of the H_2S molecules move toward the surface. One of them changed its initial configuration with two H atoms pointing to the surface and the distance between one H atom of H_2S and the surface O atom is 1.89 Å (shown in Figure 7c), whereas the other H_2S stays on top of Ni atom paralleling to the surface with S−Ni bond length 2.59 Å. The molecule angle of these H_2S are changed slightly from the free gas molecule (89.53° and 92.88°), respectively. The remaining two H_2S molecules are repelled from the surface. One H_2S molecule has one H atom pointing toward the S atom of the other H_2S molecule with the atomic distance around 3.0 Å.

To investigate the effect of H_2S molecules on the NiO surface, the electronic structure has been evaluated by plotting total and partial density of states. It is observed that band gap of the system is decreased with the increase of H_2S coverage, which is detecting parameter for gas sensing. Shape of the valence and conduction bands of the system is not much affected except closing the band gap (Figure 4b). The band gap reduction with H_2S molecules are 0.06 and 0.16 for 0.25 and 0.5 ML coverage, respectively. This small change of the band

gap will affect the conductivity of the substrate surface. In case of 1 ML, the band gap of the adsorbed system is 2.45 eV, which is almost the same as the bare NiO surface (2.48 eV). It means that H_2S molecules interact with each other rather than with the surface at high coverage. Therefore, NiO surface is sensitive to the H_2S molecule at low coverage.

For further detailed investigation of molecular interaction with the surface, we have employed the Bader analysis to calculate the charge transfer between the molecule and the surface. As H_2S is a reducing gas, charges are transferred from molecule to the surface, with $0.067e^-$, $0.050e^-$, and $0.045e^-$ charges transferred for 0.25 ML, 0.5 ML, and 1.0 ML coverage, respectively. The PDOS H_2S adsorption with 0.5 ML has been plotted in Figure 8. The interaction between the first H_2S

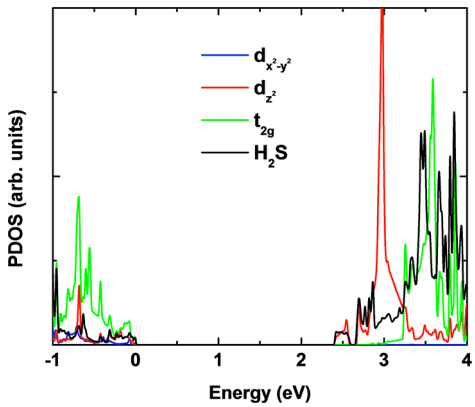

Figure 8. Partial density of states (PDOS) of surface Ni 3d states and the total density of states of H_2S molecule. Fermi energy is set to zero.

molecule with surface Ni atom comes from the overlapping of Ni atom d_{z^2} states and LUMO state of H_2S, inducing the band gap decrease. It is also explained from the isosurface charge distribution diagram that different colors indicate the charge accumulation (cyan) and depletion (yellow) (shown in Figure 9).

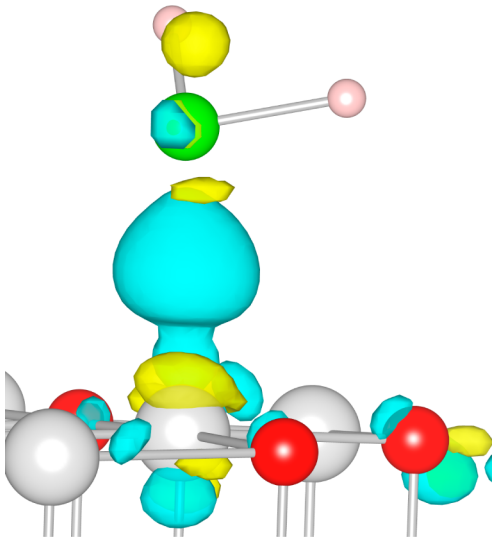

Figure 9. Isosurface of differential charge density of H_2S gas molecule adsorbed at NiO (100) surface (yellow, depletion; cyan, accumulation) (isovalue = 0.003 e/Å^3).

Adsorption of NH_3. The adsorption of NH_3 molecules at NiO (100) surface is studied by calculating the energetic and electronic properties. The stable adsorption site for NH_3 is on the top of the Ni atom at the surface. The bond length of N atom of molecule and surface Ni atom is 2.11 Å after the atomic optimization. The NH_3 molecule adsorption on NiO (100) surface is also found to be exothermic process with adsorption energies of −0.33, −0.27, and −0.101 eV per molecule for 0.25, 0.5, and 1 ML coverage, respectively. At 0.25 ML, the molecular plane determined by the three H atoms is slightly tilted forming a small angle with surface plane. The N−H bond length (1.22 Å) does not change as compared to free molecule. It is noted that the surface Ni atom moves slightly out of the surface plane (0.15 Å) to bind with the N atom. At 0.5 ML, both NH_3 molecules have the same adsorption configuration. The stable adsorption site is also on top of the Ni atom with the (Ni−N) bond length of 2.20 Å. The bond length of N−H becomes 1.02 Å smaller than the free molecule 1.22 Å, which may be due to the interaction between the NH_3 molecules. The molecular plane containing hydrogen atoms are tilted together with the geometry change shown in Figure 10. The interaction of

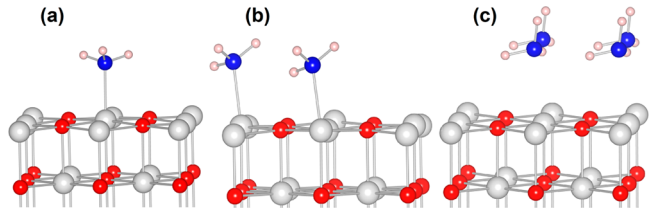

Figure 10. Adsorption of NH_3 molecules adsorbed on NiO (100) surface with different coverage: (a) 0.25 ML, (b) 0.5 ML, and (c) 1 ML after relaxation. Ni, O, N, and H atoms are represented by gray, red, blue, and white spheres, respectively.

monolayer NH_3 with surface has also been investigated. The bond length of the surface Ni atom and N atom of molecule is 2.64 Å, which is much larger than the lower coverage and the adsorption energy also decreases, which might originate from the interaction between NH_3 molecules.

The total and partial density of states have been plotted to elaborate the adsorption phenomena and the effect on the electronic structure of the system. Optical band gap of the NiO surface is reduced by the adsorption of NH_3 molecule by 0.24, 0.72, and 0.54 eV for 0.25, 0.5, and 1 ML coverage, respectively (shown in Figure 4c). Band gap reduction clearly reflects the adsorption energies. It indicates that the NiO (100) surface is more sensitive for NH_3 gas as compared to the H_2S gas. The charge transfer has been calculated by Bader analysis, which is shown that $0.067e^-$, $0.066e^-$, and $0.040e^-$ charges has been transferred from the molecule to the surface for 0.25 ML, 0.5 ML, and 1.0 ML coverage, respectively. For detailed investigation of adsorption mechanism, partial density of states of NH_3 and surface Ni atoms are plotted in Figure 11. It indicates that NH_3 HOMO (highest occupied molecular orbital) level with Ni d_{z^2} states contribute to the interaction of molecule with surface. Isosurface of differential charge density shows that the increased charge density between N and surface Ni atoms indicates the interaction of N p_z state and Ni atom d_{z^2}. The N p_z states have also some charge exchange with Ni d_{xy} and d_{yz} states. After optimization, charges flow from H atom to N atom, due to the geometry change of the initial position of NH_3 molecule, Isosurface of differential charge

dx.doi.org/10.1021/am3016894 | ACS Appl. Mater. Interfaces 2012, 4, 5691−5697

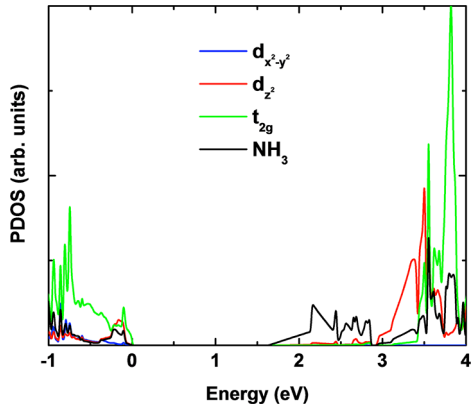

Figure 11. Partial density of states (PDOS) of surface Ni 3d states and the total density of states of NH_3 molecule. Fermi energy is set to zero.

density clearly indicates the charge depletion (yellow) and charge accumulation (cyan), which is shown in Figure 12.

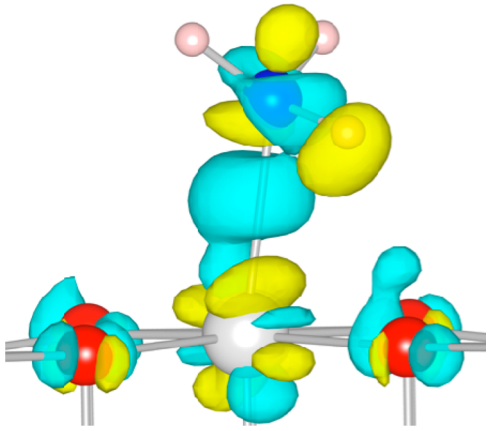

Figure 12. Isosurface of differential charge density of NH_3 gas molecule adsorbed at NiO (100) surface (yellow, depletion; cyan, accumulation) (isovalue = 0.003 e/Å^3).

To further understand the effect of the adsorbed molecular on the NiO bare surface, we have calculated the work function of the adsorbed system shown in Figure 13. At high coverage the gas molecular introduces a net dipole moment which will change the chemical sensing properties of the surface.[33−35] Moreover, the detected conductivity change is close related to the shift of work function for the largely chemisorbed layers with charge transfer between surface and molecular.[36] In the conventional method, the work function (vacuum level) could be calculated as $\phi = V(\infty) - E_F$, where $V(\infty)$ and E_F are the electrostatic potential in a vacuum region far from the neutral surface and the Fermi energy of the neutral surface system, respectively.[37,38] The calculated work function of NO_2 adsorption has hill-shaped behavior. At low coverage, the work function is smaller than that of NiO bare surface, about 0.46 eV smaller. At half monolayer, the work function increased to 5.86 eV which is 0.8 eV larger than bare surface. The work function decreased to 4.02 eV at monolayer coverage. The adsorbed NO_2 molecular at half-monolayer coverage induced a lager work function as compared to the bare surface. From the optimized adsorption configuration, the two NO_2 molecular pointing to the same direction and arranged orderly at the surface. It will give rise to the net dipole moment of the surface.

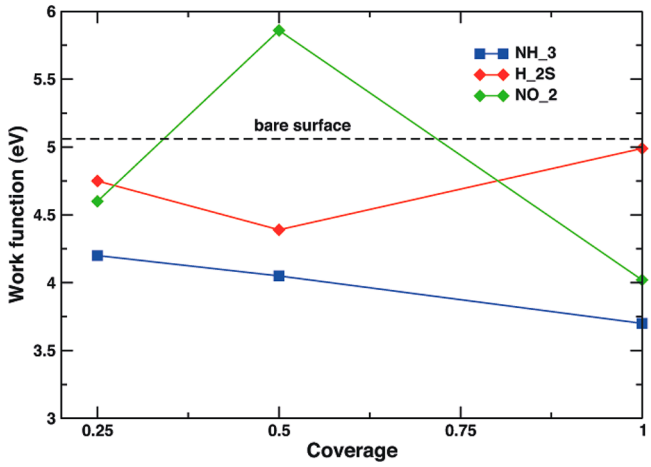

Figure 13. Calculated work function of bare NiO (100) surface and the work function of different molecular adsorption at different coverage.

Here a gas molecular is modeled as a point dipole. According to Helmholtz equation, the potential drop, $e\Delta\Phi$, and the gas-phase molecular dipole P_0, have the following equation

$$e\Delta\Phi = 4\pi\frac{NP_0\cos\theta}{A\varepsilon} \quad (2)$$

where A is the surface area, N is the number of molecules, θ is the molecular tilt angle, ε is the dielectric constant of the orderly arranged gas molecular monolayer, and centimeter-gram-seconds (cgs) units are used. Our results can be explained within this model. At half monolayer coverage, the increased of the net dipole moment leads to a larger work function with respect to bare surface. At high coverage, the work function is decreased because of the depolarization effect[39] as the four NO_2 arranging disorderly on the surface with net dipole moment decreased.

When H_2S adsorbed on surface, the work function has a valley-shaped behavior. The work function first decreases to the minimum value at half monolayer coverage as the increase of the net dipole moment. Compared with NO_2 adsorption, we infer that the dipole moment of H_2S on surface has opposite direction. It is also consistent with the different charge transfer mechanism of the two gases adsorption as discussed above. At monolayer coverage, the work function increases to 5.0 eV, which is approaching very closely to bare surface. After optimization, the four H_2S molecular are distributed disorderly on the surface, which leads to decrease of the net dipole moment. Therefore, the change of the work function can also attribute to the depolarization effect.[39]

The work function decreases as the coverage increases for the NH_3 molecules which behaves differently as compared to the other two molecules. From the optimized structure, we notice that the NH_3 arranged orderly at different coverages and the density of the dipole moment increases as the coverage increase. Thus the change in work function with respect to the coverage is high.

CONCLUSIONS

In conclusion, we have performed the first-principle calculations to evaluate the adsorption energies, electronic structure and charge transfer mechanism for describing the adsorption behavior of NO_2, H_2S and NH_3 molecules on NiO (100)

surface at different coverage. Chemisorption interaction of NO_2 molecule with NiO surface is very strong as compared to the H_2S and NH_3 molecules, which indicate that it is very difficult to remove NO_2 molecule from the surface. Therefore, the sensing response is low. At high coverage, reactive sites are saturated; half of NO_2 molecules do not interact with surface and form a second ad-layer. The concentration of unoccupied states in the band gap has been increased by the rising of the molecular coverage, which gives the high electronic conductivity. As the H_2S adsorbed on NiO (100) surface, the band gap of the adsorbed system decreases with coverage up to 0.5 ML coverage. The adsorption of NH_3 is slightly different with that of H_2S. The adsorption energy increases with the coverage and the band gap is reduced. Charge transfer between gas molecular and NiO surface has been calculated by bader analysis. For oxidizing gas molecular NO_2, charges are transferred from surface to molecular. Although for the reducing gas molecular H_2S and NH_3, charges are transferred from molecular to surface. The binding mechanism between surface and adsorbed molecular has been illustrated by plotting isosurface charge distribution which shows that the main interaction between surface and gas molecular is the 3d states of surface Ni atom and the HOMO and LUMO states of the molecular. To further understand the effect of gas adsorption on the bare NiO surface, we have performed work function calculations. The work function of NO_2 adsorption has hill-shaped behavior. The work function first increases with coverage increase and decreases at monolayer coverage as a result of depolarization effect. For H_2S adsorption, the work function is decreased at first as a different dipole moment is formed at surface with respect to NO_2 adsorption. The adsorption NH_3 gas on surface induces a smaller work function and the work function decreases as the coverage increase. Our results suggest a better understanding of gas-sensing mechanism of NiO surface toward NO_2, H_2S, and NH_3 gases.

AUTHOR INFORMATION

Corresponding Author

*E-mail: baochang@kth.se.

Notes

The authors declare no competing financial interest.

ACKNOWLEDGMENTS

We acknowledge the Swedish Research Council (VR and FORMAS) for financial support. B.C.W. thanks the Chinese Scholarship Council (CSC) and J.N. is thankful to the Higher Education Commission (HEC) of Pakistan. SNIC and UPPMAX are acknowledged for providing computing time.

REFERENCES

(1) Eiyama, T.; Kato, A.; Fujiishi, K.; Nagatani, M. *Anal. Chem.* **1962**, *34*, 1502−1503.

(2) Batzill, M.; Diebold, U. *Phys. Chem. Chem. Phys.* **2007**, *9*, 2307−2318.

(3) Kamal, H.; Elmaghraby, E. K.; Ali, S. A.; Abdel-Hady, K. *J. Cryst. Growth.* **2004**, *262*, 424−434.

(4) Choi, J. M.; Im, S. *Appl. Surf. Sci.* **2005**, *244*, 435−438.

(5) Luyo, C.; Ionescu, R.; Reyes, L. F.; Topalian, Z.; Estrada, W.; Llobet, E.; Granqvist, C. G.; Heszler, P. *Sens. Actuators, B* **2009**, *138*, 14−20.

(6) Hotovy, I.; Rehacek, V.; Siciliano, P.; Capone, S.; Spiess, L. *Thin Solid Films* **2002**, *418*, 9−15.

(7) Hotovy, I.; Huran, J.; Siciliano, P.; Capone, S.; Spiess, L.; Rehacek, V. *Sensor Actuat B-Chem.* **2001**, *78*, 126−132.

(8) Hotovy, I.; Huran, J.; Spiess, L.; Capkovic, R.; Hascik, S. *Vacuum* **2000**, *58*, 300−307.

(9) Imawan, C.; Solzbacher, F.; Steffes, H.; Obermeier, E. *Sens. Actuators, B* **2000**, *68*, 184−188.

(10) Hotovy, I.; Huran, J.; Siciliano, P.; Capone, S.; Spiess, L.; Rehacek, V. *Sens. Actuators, B* **2004**, *103*, 300−311.

(11) Cantalini, C.; Post, M.; Buso, D.; Guglielmi, A.; Martucci, A. *Sens. Actuators, B* **2005**, *108*, 184−192.

(12) Brilis, N.; Foukaraki, C.; Bourithis, E.; Tsamakis, D.; Giannoudakos, A.; Kornpitsas, M.; Xenidou, T.; Boudouvis, A. *Thin Solid Films* **2007**, *515*, 8484−8489.

(13) Stamataki, M.; Tsamakis, D.; Brilis, N.; Fasaki, I.; Giannoudakos, A.; Kompitsas, M. *Phys. Status Solidi A* **2008**, *205*, 2064−2068.

(14) Dirksen, J. A.; Duval, K.; Ring, T. A. *Sens. Actuators, B* **2001**, *80*, 106−115.

(15) Lee, C. Y.; Chiang, C. M.; Wang, Y. H.; Ma, R. H. *Sens. Actuators, B* **2007**, *122*, 503−510.

(16) Spencer, M. J. S. *Prog. Mater. Sci.* **2012**, *57*, 437−486.

(17) Fine, G. F.; Cavanagh, L. M.; Afonja, A.; Binions, R. *Sensors-Basel* **2010**, *10*, 5469−5502.

(18) Liechtenstein, A. I.; Anisimov, V. I.; Zaanen, J. *Phys. Rev. B* **1995**, *52*, R5467−R5470.

(19) Dudarev, S. L.; Botton, G. A.; Savrasov, S. Y.; Humphreys, C. J.; Sutton, A. P. *Phys. Rev. B* **1998**, *57*, 1505−1509.

(20) Rohrbach, A.; Hafner, J.; Kresse, G. *Phys. Rev. B* **2004**, *69*, 075413.

(21) Rohrbach, A.; Hafner, J. *Phys. Rev. B* **2005**, *71*, 045405.

(22) Blochl, P. E. *Phys. Rev. B* **1994**, *50*, 17953−17979.

(23) Kresse, G.; Hafner, J. *Phys. Rev. B* **1993**, *47*, 558−561.

(24) Kresse, G.; Hafner, J. *Phys. Rev. B* **1994**, *49*, 14251−14269.

(25) Kresse, G.; Joubert, D. *Phys. Rev. B* **1999**, *59*, 1758−1775.

(26) Perdew, J. P.; Chevary, J. A.; Vosko, S. H.; Jackson, K. A.; Pederson, M. R.; Singh, D. J.; Fiolhais, C. *Phys. Rev. B* **1992**, *46*, 6671−6687.

(27) Monkhorst, H. J.; Pack, J. D. *Phys. Rev. B* **1976**, *13*, 5188−5192.

(28) Netzer, F. P.; Prutton, M. *J. Phys. C Solid State* **1975**, *8*, 2401−2412.

(29) Weltoncook, M. R.; Prutton, M. *J. Phys. C Solid State* **1980**, *13*, 3993−4000.

(30) Dudarev, S. L.; Liechtenstein, A. I.; Castell, M. R.; Briggs, G. A. D.; Sutton, A. P. *Phys. Rev. B* **1997**, *56*, 4900−4908.

(31) Nisar, J.; Araujo, C. M.; Ahuja, R. *Appl. Phys. Lett.* **2011**, *98*, 083115.

(32) Nisar, J.; Araujo, C. M.; Ahuja, R. *Surf. Sci.* **2010**, *604*, 617−622.

(33) Paska, Y.; Stelzner, T.; Christiansen, S.; Haick, H. *ACS Nano* **2011**, *5*, 5620−5626.

(34) Heimel, G.; Romaner, L.; Bredas, J.; Zojer, E. *Phys. Rev. Lett.* **2006**, *96*, 196806.

(35) Natan, A.; Kronik, L.; Haick, H.; Tung, R. *Adv. Mater.* **2007**, *19*, 4103−4117.

(36) Barsan, N.; Koziej, D.; Weimar, U. *Sens. Actuators, B* **2007**, *121*, 18−35.

(37) Kajita, S.; Nakayama, T.; Yamauchi, J. *J. Phys. Conf. Ser.* **2006**, *29*, 120−123.

(38) Nisar, J.; Wang, B.; Araujo, C.; Silva, A.; Kang, T.; Ahuja, R. *Int. J. Hydrogen Energy* **2012**, *37*, 3014.

(39) Natan, A.; Zidon, Y.; Shapira, Y.; Kronik, L. *Phys. Rev. B* **2006**, *73*, 193310.